Plant Cell Physiol. 59(7): 1300–1308 doi:10.1093/pcp/pcy054
available online at www.pcp.oxfordjournals.org

Biochemical, structural, and physiological characteristics of vacuolar H^+-pyrophosphatase

Shoji Segami[1], Mariko Asaoka[1,2], Satoru Kinoshita[1], Mayu Fukuda[1], Yoichi Nakanishi[1], and Masayoshi Maeshima[1]

[1] Laboratory of Cell Dynamics, Graduate School of Bioagricultural Sciences, Nagoya University, Nagoya 464-8601, Japan
[2] Department of Biology, Tokyo Gakugei University, Nukui Kitamachi 4-1-1, Koganei-shi, Tokyo 184-8501, Japan

*Corresponding author: Masayoshi Maeshima,
E-mail, maeshima@agr.nagoya-u.ac.jp

Abbreviations: GFP, green fluorescent protein; H^+-PPase, proton-translocating inorganic pyrophosphatase; mGFP, monomer type GFP; PPi, inorganic pyrophosphatase; UTP, uridine 5'-triphosphate; V-ATPase, vacuolar proton-translocating adenosine triphosphatase; V-PPase, vacuolar H^+-PPase.

Abstract
Proton-translocating inorganic pyrophosphatase (H^+-PPase) actively translocates protons across membranes coupled with the hydrolysis of inorganic pyrophosphate (PPi). H^+-PPase, which is composed of a single protein and uses a simple compound as a substrate, has been recognized as a new type of ion pump in addition to the P-, F-, and V-type ion translocating ATPases. H^+- and Na^+-PPases are distributed in various organisms including plants, parasitic protozoa, Archaebacteria, and bacteria, but are not present in animals or yeast. Vacuolar H^+-PPase has dual functions in plant cells: hydrolysis of cytosolic PPi to maintain the levels of PPi and translocation of protons into vacuoles to maintain the acidity of the vacuolar lumen. Acidification performed with the vacuolar type H^+-ATPase and H^+-PPase is essential to maintain acidic conditions, which are necessary for vacuolar hydrolytic enzymes and for supplying energy to secondary active transporters. Recent studies using loss-of-function mutant lines of H^+-PPase and complementation lines with soluble PPases have emphasized the physiological importance of the scavenging role of PPi. An overview of the main features of H^+-PPases present in the vacuolar membrane is provided in terms of tissue distribution in plants, intracellular localization, structure-function relationship, biochemical potential as a proton pump, and functional stability.

Keywords: H^+-pyrophosphatase • Proton pump • Pyrophosphate • Structure-function relationship • 3-D structure • Vacuolar acidification

Introduction

H^+-translocating inorganic pyrophosphatase (H^+-PPase) actively transports protons from the cytosol across membranes coupled with the hydrolysis of inorganic pyrophosphate (PPi). H^+-PPase is composed of a single protein with a molecular mass of approximately 70–80 kDa (Maeshima 2000). The enzymatic activity of pyrophosphatase was first detected as PPi synthase in chromophore membranes of the purple photosynthetic bacteria *Rhodospirillum rubrum* (Baltscheffsky 1967). Subsequently, the enzyme was solubilized from the membrane and characterized as an enzyme with PPi hydrolysis activity (Nyren et al. 1984). PPi-dependent proton transport activity in plant vacuolar membranes was first reported in the 1980s (Chanson et al. 1985, Rea and Poole 1986, Takeshige et al. 1988). H^+-PPase was isolated from the vacuolar membranes of *Vigna radiata* hypocotyls (Maeshima and Yoshida 1989) and cDNA encoding the *Arabidopsis thaliana* enzyme was cloned (Sarafian et al. 1992).

H^+-PPase has been identified in plants, parasitic protozoa, Archaebacteria, and bacteria, but not in animals or fungi (Seufferheld et al. 2011). Bacteria, including *Agrobacterium radiobacter* and the hyperthermophilic bacteria *Thermotoga maritima* and *Carboxydothermus hydrogenoformans*, also express H^+-PPase (Perez-Castineira 2001, Belogurov and Lahti 2002, Seufferheld et al. 2011). H^+-PPase has been recognized as a new type of ion pump, in addition to F-type (e.g. mitochondrial ATP synthase), V-type (e.g. vacuolar H^+-ATPase), and P-type (e.g. plasma membrane H^+- and Ca^{2+}-ATPase) ATPases (Breton and Brown 2013, Forgac 2007, Junge and Nelson 2015, Palmgren and Nissen 2011, Pedersen 2007).

H^+-PPase has two physiological roles in plants: hydrolysis of PPi in the cytosol and acidification of vacuoles. PPi is generated through many macromolecule biosynthesis reactions, such as DNA and RNA polymerization, as well as protein and cellulose synthesis (Heinonen 2001, Ferjani et al. 2014). Physiological roles of vacuolar H^+-PPase (hereafter, V-PPase) in PPi hydrolysis and vacuolar acidification during development and growth of plants have been reported in a number of studies. These studies provide additional information on the physiological significance of V-PPase (Bak et al. 2013, Ferjani et al. 2011, Gaxiola et al. 2007, Gaxiola et al. 2016, Schumacher 2014, Shen et al. 2013, Schilling et al. 2014, Maeshima 2001, Martinoia et al. 2007, Wang et al. 2016), and will not be discussed further. The aim of this review is to provide a general overview, linking molecular structure, quantitative activity, and tissue-specific distribution.

Intracellular localization and tissue-specific distribution of H^+-PPases

Most plants have two types of H^+-PPases: type I and type II (Drozdowicz et al. 2000). The type I H^+-PPase requires K^+ for maximal enzyme activity and functions together with H^+-ATPase in vacuolar membranes, in which H^+-PPase accounts for approximately 10% of the vacuolar membrane protein in young tissues (Maeshima 2001). The type II H^+-PPase, which does not require K^+, is localized in the membrane of the Golgi apparatus (Mitsuda et al. 2001b, Segami et al. 2010). The amount of type II enzyme in the total membrane fraction is approximately less than 0.3% of the

type I H^+-PPase (Segami et al. 2010). Therefore, type I H^+-PPase is the primary H^+-PPase in the vacuolar membrane (V-PPase).

Several groups have reported the plasma membrane localization of V-PPase based on immune electron and immunofluorescence microscopy (Long et al. 1995, Robinson 1996, Langhans et al. 2001, Li et al. 2005, Paez-Valencia et al. 2011, Regmi et al. 2016). In general, non-specific interaction of an antibody is a common problem in immunohistochemical analyses. Visualization of the target protein linked with a fluorescent protein such as green fluorescent protein (GFP) also has artifactual concerns: namely, abnormal localization of the target protein and side effects caused by overexpression of the GFP-linked protein (Grenfen et al. 2010). Recently, Segami et al. (2014) generated a GFP-V-PPase construct with enzyme activity by introducing GFP into the intermolecular flexible loop (loop *a*) that faces the cytoplasm. They used a monomer-type GFP (mGFP) instead of the regular GFP, which has a tendency to form GFP dimers in cells. V-PPase-mGFP was recovered in the same fraction as the endogenous V-PPase. The careful experiments in this study showed that V-PPase localizes to the vacuolar membrane but not the plasma membrane of most cells, including the sieve element-companion cell. Figure 1 shows the typical localization of V-PPase in the vacuolar membrane in elongating root cells of *A*. *thaliana*. Thus, it is reasonable to conclude that V-PPase functions only in the vacuolar membrane of all cells.

V-PPase is distributed in most tissues and cells although the amount of enzyme varies with the tissue. Exceptionally, V-PPase is absent in the columella cells of *A*. *thaliana* (Segami et al. 2014), which contain starch grains and sense gravity (Chen et al. 1999, Vitha et al. 2007). On the other hand, V-PPase is very abundant in growing cells. In the case of *A*. *thaliana* etiolated seedlings, cell proliferation and elongation zones show a high protein content and enzymatic activity of V-PPase (Figure 1) (Maeshima 1990, Nakanishi and Maeshima 1998, Segami et al. 2014). Furthermore, the amount of V-PPase based on the vacuolar membrane protein in 3-d-old cotyledons was twice as that in the 10-d-old cotyledons (Segami et al. 2014). In these growing cells, a large amount of ATP is consumed to form new cells and a large amount of PPi is generated via macromolecule biosynthesis. Therefore, V-PPase likely contributes to both the removal of PPi and acidification of growing vacuoles (Maeshima 2000).

High protein accumulation of V-PPase has been reported in the shoot apical meristem, leaf primordia, vascular cambium, and ovules of *A*. *thaliana* (Segami et al. 2014), as well as for the shoot apical meristem, emergent leaf sheath, root primordium, and growing embryo of *Oryza sativa* (Regmi et al. 2016). Pollen has also been shown to exhibit high expression of the V-PPase gene in *A*. *thaliana* and *O*. *sativa*. The *A*. *thaliana* V-PPase gene (*AtVHP1*) contains a *cis*-acting element, which is specific to pollen (Mitsuda et al. 2001a). During elongation of pollen tubes, the pollen cells actively synthesize RNA, protein, and cellulose, and rapidly expand their vacuoles. In addition to growing tissues, V-PPase is abundant in organs with a high sucrose content, such as the nectary and funicle (Segami et al. 2014). Therefore, the PPi hydrolysis and proton pump functions of V-PPase are both required for

scavenging cytosolic PPi and activation of secondary active transporters in the vacuole. In contrast with the normal elongation of pollen tubes, in the case of self-incompatibility, soluble PPase, not V-PPase, is inactivated by phosphorylation in the genus *Papaver* (de Graaf 2006), indicating the importance of PPi removal for cell elongation.

A high amount of V-PPase might be related to the PPi-scavenging role (Ferjani et al. 2011, Ferjani et al. 2014). The concentration of PPi affects the amount of sucrose metabolically produced from storage lipids during germination (Ferjani et al. 2011, Takahashi et al. 2017) and photoassimilate partitioning (Lerchl 1995). For example, UDP-glucose (UDP-Glc) pyrophosphorylase, which catalyzes the reaction glucose-1-phosphate (G1P) + UTP $\leftrightarrow$ UDP-Glc + PPi, produces PPi during sucrose synthesis (Ferjani et al. 2011).

In sieve companion cells, sucrose is accumulated to high levels by the sucrose/H^+ symporter in the plasma membrane (Pizzio et al. 2015, Regmi et al. 2016). In general, the symporter is energized by the plasma membrane H^+-ATPase. The substrate ATP is supplied through glycolysis via UDP-Glc, which is generated from the hydrolysis of sucrose. UDP-Glc hydrolysis requires PPi to produce G1P and subsequently glucose 6-phosphate. Thus, PPi should be kept at high levels (Lerchl et al. 1995a). Recent reports have shown by immunochemical analysis that V-PPase is located in the plasma membrane and catalyzes the reverse reaction: synthesis of PPi using a pH gradient across the plasma membrane generated by the plasma membrane H^+-ATPase (Pizzio et al. 2015, Regmi et al. 2016, Gaxiola et al. 2016). This differs from a report that demonstrated vacuolar membrane localization of V-PPase even in companion cells using functional V-PPase-mGFP (Segami et al. 2014). However, the reverse reaction of PPi synthesis by V-PPase remains to be examined with biochemical experiments. In the case of the photosynthetic bacteria *R. rubrum*, H^+-PPase has been reported to catalyze both hydrolysis and synthesis reversibly; namely, PPi hydrolysis in the dark and PPi synthesis in the light (Baltcheffsky 1967).

Two conflicting points, H^+-PPase localization in the plasma membrane and function of H^+-PPase as a PPi synthase, are very important when discussing the physiological roles of H^+-PPases. Furthermore, severe phenotypes observed in RNAi-mediated H^+-PPase knockdown mutants (Pizzio et al. 2015) differed from the mild phenotypes observed in loss-of-function mutants in which specific amino acid(s) of V-PPase were exchanged and deleted (Ferjani et al. 2011). Discussion of these conflicting points will require information on soluble PPases and the genetic and metabolic changes in these mutant lines, which will deepen our understanding of V-PPases.

Molecular structure and diversity of H^+-PPases

Arabidopsis thaliana has one gene encoding the type I enzyme (VHP1, At1g15690, also called AVP1) and two genes encoding the type II enzymes (VHP2;1 and VHP2;2; At1g78920 and At1g16780, respectively). In comparison, *Vigna radiate*, *Hordeum vulgare*, and *Oryza sativa* have one, two, and six type I V-PPase genes,

respectively. Among the six genes in *O. sativa*, *OsVHP1;1* and *OsVHP1;2* are the major ones expressed in rice (Muto et al. 2011). These genes may be expressed in cell-, tissue-, and growth-stage specific manners in crops. The genes in *A. thaliana* and *V. radiate* probably have strong promoters, and their translation products comprise a major proportion of the vacuolar membrane proteins as mentioned above.

Plants have soluble inorganic PPases with primary structures that resemble those of the soluble PPases in *Escherichia coli* (hexametric enzyme, PPa) and *Saccharomyces cerevisiae* (dimeric enzyme, IPP) (Schulze et al. 2004, Gómez-García et al. 2006). *A. thaliana* has several PPase isoforms, and some isoforms, such as PPa1 and PPa2, were detected in the cytosol (Schulze et al. 2004, Navarro-Dela Sancha et al. 2007). The primary and tertiary structures of V-PPases in various organisms differ from those of soluble PPases in plants, yeast, and bacteria. V-PPases do not have any sequence similarity to soluble PPases, even at the catalytic site, although the both types of enzymes catalyze PPi hydrolysis (Sivula et al. 1999, Drozdowicz and Rea 2001, Lin et al. 2012). Therefore, soluble PPases and H^+-PPases including V-PPases might have evolved from different molecular ancestors.

In 2012, the tertiary structures of the V-PPase of *V. radiata* (Lin et al. 2012) and the Na^+-PPase of the hyperthermophilic bacterium *T. maritima* (Kellosalo et al. 2012) were revealed by crystallography. Figure 2 shows the structural model of the H^+-PPase homodimer as well as a schematic diagram. Prior to these studies, there were several reports on the homodimeric structure (Maeshima 1990b, Sato et al. 1991, Mimura et al. 2005), as well as the membrane topology with 16 transmembrane (TM) domains in the plant V-PPase (Mimura et al. 2004), 17 TM domains in *Streptomyces coelicolor* (Mimura et al. 2004, Hirono et al. 2005), and various functional residues (Hirono et al. 2007a, 2007b, Lee et al. 2011, Nakanishi et al. 2001, Pan et al. 2011). Crystallography has revealed the principle structure of the plant V-PPase with 16 TM helices and provided a detailed arrangement of a large number of functional amino acid residues, which were revealed by site-directed mutagenesis and heterologous expression in yeast.

Furthermore, the coupling mechanism of V-PPase was proposed from analysis of the structure-function relationship of the enzymes of *T. maritima* and *V. radiata* (Kajander et al. 2013, Li et al. 2015). Elucidation of the tertiary structure of V-PPase has provided key information for understanding the functional structure and reaction mechanism, including the transfer of energy from PPi hydrolysis to active proton translocation compared with that of F-, V-, and P-type ATPases (Breton and Brown 2013, Forgac 2007, Junge and Nelson 2015, Palmgren and Nissen 2011, Pedersen 2007). Here, we briefly introduce the structure. For a complete understanding of the detailed structure-function relationship, we recommend reading the original articles.

The plant V-PPase exists as a homodimer and the protomer contains 16 TM helices. Among the 16 TM helices, six helices (TM5, TM6, TM11, TM12, TM15, and TM16) form an inner ring that functions as the proton translocation pathway (Figure 2). The inner ring is surrounded by an outer ring composed of the remaining 10 TM helices. Several TM helices of the inner and outer rings are involved in formation of the homodimer. Most of the V-PPase TM helices are long and extend to the cytosol.

The binding sites for Mg-PPi, free Mg^{2+}, and the catalytic domain are found in the hydrolytic center, which is composed of several residues of the long TM helices of the inner ring. During the reaction, PPi hydrolysis and active proton translocation are mechanically coupled. Binding and subsequent hydrolysis of PPi triggers a conformational change, particularly with respect to the positional relationship of the TM helices (Kajander et al. 2013, Li et al. 2015). Each helix changes its angle in the membrane slightly and rotates to a small degree during the reaction. In addition, the cytoplasmic TM5/TM6 loop changes its position in the enzyme complex. These conformational changes facilitate the translocation of a proton from the cytosolic domain and the release of the proton to the vacuolar lumen. It has been suggested that the Na^{+}-PPase of *T*. *maritima* has a similar reaction mechanism (Kajander et al. 2013, Kellosalo et al. 2012, Li et al. 2015). Aspartic and glutamic acid residues in TM6 are involved in the acceptance, translocation, and release of protons. The lysine residues in TM16 push protons trapped by a glutamate residue of TM6 to the vacuolar lumen, which is accompanied by a slight shift of TM16 (Li et al. 2015). The overall reaction mechanism is unique and differs from the rotational mechanism of ATP synthase and V-ATPase as well as the marionette mechanism of P-type ion pumps such as Ca^{+}-ATPase and the plasma membrane H^{+}-ATPase (Junge and Nelson 2015, Forgac 2007, Palmgren and Nissen 2011, Pedersen 2007).

Recently, uncoupled V-PPase mutants, which exhibit PPi hydrolysis activity but no proton pump activity, were generated by site-directed mutagenesis of *V*. *radiata* V-PPase (Asaoka et al. 2014). The mutated V-PPase has a single-residue mutation of Ile-545 or Leu-749 to alanine, positioned in TM12 or TM16 of the inner ring. The cytosolic regions of TM12 and TM16 form the catalytic domain with the remaining inner ring TM helices. Both TM12 and TM16 might be involved in PPi hydrolysis as well as the mechanical coupling between PPi hydrolysis and proton translocation. Leu-749, located in TM16, supports the proton relay mechanism by the downshift during reaction (Li et al. 2015). Furthermore, when expressed in a V-PPase knockout mutant, the mutant uncoupled V-PPase exhibited normal PPi hydrolysis but no proton pump activity (Asaoka et al. 2016). From a physiological point of view, this enzyme can be used to evaluate PPi hydrolysis activity *in planta*.

Arabidopsis thaliana loss-of-function mutants of V-PPase, *fugu5*, have been used in many experiments as loss-of-function mutants (Ferjani et al. 2011). In *fugu5-1*, Ala-709, which corresponds Ala-705 in the V-PPase of *V. radiata*, was replaced with a threonine residue. Ala-705 is located on the cytosolic side of TM15, which is essential for PPi hydrolysis. In *fugu5-2*, Glu-272 (corresponding to Glu-268 of the *V. radiata* enzyme) was replaced with a lysine residue. Glu-268 is located within the cytosolic catalytic domain between TM5 and TM6. In *fugu5-3*, Ala-553 (corresponding to Ala-549 of the *V. radiate* enzyme) was replaced with a threonine residue and the five residues from Leu-554 to Ala-558 (corresponding to Leu-550 to Ala-554 of the *V. radiate* enzyme). This deleted region in TM 12 and is essential as a coupling funnel and gate (Figure 2).

V-PPase contains a flexible region, the cytoplasmic loop *a*, which has not been determined by crystallography. Here, we briefly describe the loop *a*, located between

TM1 and TM2, which is not conserved among the H^+-PPases of various organisms. Loop *a* contains many glutamate residues and is thought to be part of an intrinsically disordered structure. This property was exploited to insert GFP to enable visualization of the *A. thaliana* V-PPase. When GFP was inserted into this flexible loop *a*, the enzyme activity was retained (Segami et al. 2014). What is the biochemical role of loop *a*? Why has loop *a* been maintained during molecular evolution? Some possibilities for the biochemical role of loop *a* have been suggested. For example, loop *a* may provide movement to the TM helices, function as the ligand binding site, if any, and/or as a sensing domain of pH and salt concentrations in the cytosol.

Physicochemical roles of V-PPase in small intracellular organelles

In this section, we review the functional potential of V-PPase with respect to PPi hydrolysis and proton pumping activities. The velocity of proton translocation by V-PPase has been determined to be 14 s^{-1} per protomer by patch clamp analysis of *V. radiata* V-PPase expressed heterologously in giant vacuoles of *S. cerevisiae* (Nakanishi et al. 2003). The PPi-dependent H^+ current was stable for at least 60 min, although ATP-dependent H^+ current by the endogenous yeast V-ATPase was markedly decreased even for 200 s (Figure 3). The velocity (14 s^{-1} per protomer) was determined from the following data: PPi-dependent H^+ current (9.3 pA; 1 pA corresponds to ~6 × 10^6 H^+ s^{-1}) and the number of enzymes in a vacuole (4.2 × 10^6 protomers). Since V-PPase exists as a homodimer (Lin et al. 2012, Sato et al. 1991), the molecular activity of the dimer is calculated to be 28 s^{-1} (Nakanishi et al. 2003). The rate of PPi hydrolysis can be calculated from the activity of a purified preparation of *V. radiata* (8.45 units/mg) and molecular mass of 80,919 Da (Maeshima and Yoshida 1989, Nakanishi and Maeshima 1998). The calculated turnover of PPi hydrolysis was 23 s^{-1} $dimer^{-1}$. A small portion of the purified V-PPase may have been inactivated during purification. The similarity in the rate of proton transport (28 s^{-1} $dimer^{-1}$) and PPi hydrolysis (23 s^{-1} $dimer^{-1}$) indicates an H^+/PPi stoichiometry of 1.

Ion transport across the membrane in plants performs two physiological roles. First, a large amount of ions are transported to support plant growth as nutritional elements; second, the concentration gradients of ions are generated to maintain cellular function. As an example of the first role, major nutrients, including NO_3^-, NH_4^+, K^+, Ca^{2+}, Mg^{2+}, PO_4^{3-}, and SO_4^{2-}, are translocated across the plasma membrane and membranes of intracellular organelles. Proton translocation is an example of the second role, and in most cases, the absolute amount of protons is not large.

Here, we calculate the capacity of V-PPase in a model vacuole with a diameter of 10 μm (Figure 4). The volume is calculated to be 5.2 × 10^{-13} L. If the luminal pH is 7.0, the vacuole contains 3.2 × 10^4 protons (1.0 × 10^{-7} M). At pH 6.0, the number of protons is 3.2 × 10^5. To decrease the vacuolar pH from 7.0 to 6.0, the proton pump must translocate 2.9 × 10^5 protons into the vacuole. Is it possible for V-PPase to

translocate the calculated number of protons? In the case of giant yeast cells expressing *V. radiata* V-PPase, the number of enzymes in the membrane of a vacuole with a diameter of 16.8 μm was determined to be 4.2×10^6 molecules (Nakanishi et al. 2003). If this number is applied to a vacuole with a diameter of 10 μm, the enzyme number is calculated to be 1.5×10^6 protomers and 7.5×10^5 dimers. Indeed, V-PPase occupies 10% of the total weight of vacuolar membrane proteins in growing cells (Maeshima 2001). From these observations and calculations, it has been estimated that a plant vacuole with a diameter of 10 μm contains 10^5–10^6 V-PPase homodimers. As described above, the proton translocation velocity of the V-PPase dimer is 28 s^{-1}. Theoretically, 10^5 V-PPase dimers can translocate 2.9×10^6 H^+ s^{-1}, which is ten times of the amount required to acidify the vacuole from pH 7.0 to 6.0. Thus, V-PPase can acidify the vacuole to pH 6.0 within 1 s. It is worth considering the possibility that a large amount of V-PPase is present in the vacuolar membrane. Each dimer occupies 72 nm^2 of the membrane surface (Lin et al. 2012). Thus, it has been calculated that 10^5 or 10^6 V-PPase dimers occupy 2.3% or 23% of the membrane surface of a vacuole with a diameter of 10 μm.

In living cells, the rate of proton translocation decreases as the pH gradient across the membrane increases. Furthermore, several vacuolar active transporters use a pH gradient across the vacuolar membrane and as a result the pH gradient decreases in living plant cells. The purpose of this section was to explain that the molecular activity of V-PPase determined from experimental data is sufficient to acidify the vacuolar lumen quickly and maintain the acidic conditions.

Role of V-PPase in vacuole acidification in cooperation with V-ATPase

Finally, we describe the physiological roles of V-PPase, especially with respect to the acidification of vacuoles, in relation to V-ATPase, which translocates protons coupled with the hydrolysis of ATP (Gibbs free energy change, 30.5 kJ mol^{-1}). The H^+/ATP ratio is 2. Thus, the theoretical potential for acidification by V-PPase (Gibbs free energy change of PPi, 19.2 kJ mol^{-1}; H^+/PPi ratio, 1) is slightly higher than that of V-ATPase.

In addition to the plant vacuole, acidocalcisomes possess V-ATPase and V-PPase on their single membranes. Acidocalcisomes are small acidic organelles less than 0.5 μm in diameter, which accumulate PPi and polyphosphate, and are found in bacteria, protists, and animal eggs (Docampo and Moreno 2012, Seufferheld et al. 2011). Several lysosome-related organelles, such as melanosomes and lytic granules in lymphocytes in mammals, exhibit similar properties as acidocalcisomes (Docampo and Moreno 2012, Seufferheld et al. 2011). Both V-PPase and V-ATPase might be required to provide energy for many secondary active transporters including Ca^{2+}/H^+, Na^+/H^+, and Zn^{2+}/H^+ exchangers, and the phosphate transporter.

It is often considered common knowledge that V-PPase and V-ATPase are essential for acidification of plant vacuoles. Some groups have reported that overexpression of V-PPase markedly stimulated growth and increased tolerance to biotic and abiotic stresses of *A. thaliana* and many other crops (Gaxiola et al. 2012,

Hernández et al. 2016). Another group also reported that the shoot fresh weight of plants overexpressing V-PPase increased by 18–30% compared with wild-type plants at the late stage of vegetative growth (Asaoka et al. 2016). However, loss-of-function mutants of V-PPase exhibited wild-type growth at the early vegetative growth stage under normal growth conditions, although the typical phenotype of cotyledon shape and a slight increase in vacuolar pH were detected (Ferjani et al. 2011, Kriege et al. 2015).

Loss of V-ATPase shows a more severe effect on plant growth and vacuolar pH compared with the V-PPase loss-of-function mutant (Kriegel et al. 2015). From the phenotypic properties of knockout mutants, the physiological significance of V-ATPase is emphasized as described above. Remarkable phenotypes of the V-PPase loss-of-function mutant were reported for specific conditions, such as cold treatment (Kriegel et al. 2015) and growth in the absence of ammonium (Fukuda et al. 2016). In knockout mutant plants, the expression of other genes or enzymes might be induced to adapt to the loss of the target gene and to support survival. In terms of PPi hydrolysis, the physiological importance of the removal of cytosolic PPi by V-PPase has been revealed in relation to macromolecule biosynthesis, lipid metabolism, and sucrose synthesis (Ferjani et al. 2011, Fukuda et al. 2016, Takahashi et al. 2017).

Furthermore, the toxicity of PPi in cells should be considered: PPi easily forms insoluble complexes with Mg^{2+} or Ca^{2+}, which may cause damage to the cell. With respect to the physiological roles of V-PPase, soluble PPases, which also hydrolyze cytosolic PPi, should be considered. In relation to disease, many protozoa, such as *Trypanosoma brucei* and *Plasmodium falciparum*, also contain H^+-PPases and are causative microorganisms of sleeping sickness and malaria, respectively. Therefore, specific inhibitors of V-PPase might be useful in the development of novel therapeutic compounds (Hirono et al. 2003).

Our understanding of the physiological and biochemical properties of the V-PPase has been improved markedly in the past decade. Further studies will provide useful information for the fields of general molecular biology, bioenergetics, plant physiology, crop science, and pharmacology.

Funding

This work was supported by JSPS KAKENHI grant numbers 26252011 and 16H01235 to M.M, and 2816K18687 to S.S. M.F. received Research Fellowship for Young Scientists (doctoral course students).

References

Asaoka, M., Segami, S., and Maeshima, M. (2014) Identification of the critical residues for the function of vacuolar H^+-pyrophosphatase by amino acid screening based on the 3D structure. *J. Biochem.* 156: 333–344.

Asaoka, M., Segami, S., Ferjani, A., and Maeshima, M. (2016) Contribution of PPi-hydrolyzing function of vacuolar H^+-pyrophosphatase in vegetative growth of *Arabidopsis*: Evidenced by expression of uncoupling mutated enzymes. *Front. Plant Sci*., 7: article 415.

Bak, $G^·$, Lee, E.J., Lee, Y., Kato, M., Segami, S., Heven, S., et al. (2013) A role of phosphatidylinositol 3,5-bisphosphate in vacuolar structure change in guard cells of closing stomata. *Plant Cell* 25: 2202–2216. doi:10.

Baltscheffsky, M. (1967) Inorganic pyrophosphate as an energy donor in photosynthetic and respiratory electron transport phosphorylation systems. *Biochem. Biophys. Res. Commun.* 28: 270–276.

Belogurov, G., and Lahti, R. (2002) A lysine substitute for K^+: A460K mutation elimates K^+ dependence in H^+-pyrophosphtatase of *Carboxydothermus hydrogenoformans*. *J. Biol. Chem.* 277: 49651–49654.

Breton, S., and Brown, D. (2013) Regulation of luminal acidification by the V-ATPase. *Physiol.* 28: 318-329.

Chanson, A., Fichmann, J., Spear, D., and Taiz, L. (1985) Pyrophosphate-driven proton transport by microsomal membranes of corn coleoptiles. *Plant Physiol.* 79: 159–164.

Chen, R., Rosen, E., and Masson, P.H. (1999) Gravitropism in higher plants. *Plant Physiol.* 120: 343-350.

de Graaf, B.H.J., Rudd, J.J., Wheeler, M.J., Perry, R.M., Bell, E.M., Osman, K., et al. (2006) Self-incompatibility in *Papaver* targets soluble inorganic pyrophosphatases in pollen. *Nature* 444: 490–493.

Docampo, R., and Moreno, S.N.J. (2012) Acidocalcisomes. *Cell Calcium* 50: 113–119.

Drozdowicz, Y.M., Kissinger, J.C., and Rea, P.A. (2000) AVP2, a sequence-divergent, K^+-insensitive H^+-traslocating inorganic pyrophosphatase from Arabidopsis. *Plant Physiol.* 123: 353–362.

Drozdowicz, Y.M. and Rea, P.A. (2001) Vacuolar H^+ pyrophosphatases from the evolutionary backwaters into the mainstream. *Trends. Plant Sci.* 6: 206–211.

Ferjani, A., Segami, S., Horiguchi, G., Muto, Y., Maeshima, M., and Tsukaya, H. (2011) Keep an eye on PPi: the vacuolar-type H^+-pyrophosphatase regulates postgerminative development in *Arabidopsis*. *Plant Cell* 23: 2895–2908.

Ferjani, A., Segami, S., Asaoka, M., and Maeshima, M. (2014) Regulation of PPi levels through vacuolar membrane H^+-pyrophosphatase. *In* Progress in Botany, Vol. 75, ed. Lüttge, U., Beyschlag, W., and Cushman, J., pp. 145-166, Springer-Verlag, Heidelberg.

Forgac, M. (2007) Vacuolar ATPases: rotary proton pumps in physiology and pathophysiology. *Nature Rev. Mol. Cell Biol.* 8: 917-929.

Fukuda, M., Segami, S., Tomoyama, T., Nakanishi, Y., Gunji, S., Ferjani, A., et al.

(2016) Lack of H^+-pyrophosphatase causes developmental damage in *Arabidopsis* leaves in ammonia-free culture medium. *Front. Plant Sci*., 7, Article 819.

Gaxiola, R.A., Palmgren, M.G., and Schumacher, K. (2007) Plant proton pumps. *FEBS Lett.* 581: 2204–2214.

Gaxiola, R.A., Sanchez, C.A., Paez-Valencia, J., Ayre, B.G., and Elser, J.J. (2012). Genetic manipulation of a ''vacuolar'' H^+-PPase: from salt tolerance to yield enhancement under phosphorus-deficient soils. *Plant Physiol.* 159: 3–11.

Gaxiola, R.A., Regmi, K., Paez-Valencia, J., Pizzio, G., and Zhang, S. (2016) Plant H^+-PPases: reversible enzymes with contrasting functions dependent on membrane environment. *Mol. Plant* 9: 317–319.

Gómez-García, M.R., Losada, M., and Serrano, A. (2006) A novel subfamily of monomeric inorganic pyrophosphatases in photosynthetic eukaryotes. *Biochem. J.* 395: 211–221.

Grefen, C., Donald, N., Hashimoto, K., Kudla, J., Schumacher, K., and Blatt, M.R.. (2010) A ubiquitin-10 promoter-based vector set for fluorescent protein tagging facilitates temporal stability and native protein distribution in transient and stable expression studies. *Plant physiol.* 64: 355-365.

Heinonen, J.K. (2001) Biological role of inorganic pyrophosphate. Springer US, Boston, MA.

Hernández, A., Herrera-Palau, R., Madroñal, J.M., Albi, T., López-Lluch, G., Perez-Castiñeira, J.R., et al. (2016) Vacuolar H^+-pyrophosphatase AVP1 is involved in amine fungicide tolerance in *Arabidopsis thaliana* and provides tridemorph resistance in yeast. *Front. Plant Sci.* 7: 85.

Hirono, M., Ojika, M., Mimura, H., Nakanishi, Y., and Maeshima, M. (2003) Acylspermidine derivatives isolated from a soft coral *Sinularia* sp. inhibits plant vacuolar H^+-pyrophosphatase. *J. Biochem*. 133, 811–816.

Hirono, M., Mimura, H., Nakanishi, Y., and Maeshima, M. (2005) Enzymatic and molecular properties of H^+-pyrophosphatase of *Streptomyces coelicolor* expressed in *Escherichia coli. J. Biochem*. 138: 183–191.

Hirono, M., Nakanishi, Y., and Maeshima, M. (2007a) Essential amino acid residues in the central transmembrane domains for energy coupling of the H^+-pyrophosphatase of *Streptomyces coelicolor* A3(2) determined by random and site-directed mutagenesis. *Biochim. Biophys. Acta - Bioenergetics* 1767: 930–939.

Hirono, M., Nakanishi, Y., and Maeshima, M. (2007b) Identification of amino acid residues participating in the energy coupling and proton transport of *Streptomyces coelicolor* A3(2) H^+-pyrophosphatase. *Biochim. Biophys. Acta – Bioenergetics* 1767: 1401–1411.

Junge, W., and Nelson, N. (2015) ATP synthase. *Annu. Rev. Biochem*. 2015. 84: 631–657.

Kajander, T., Kellosalo, J., and Goldam A. (2013) Inorganic pyrophosphatase: one substrate, three mechanisms. *FEBS Lett.* 587: 1863–1869.

Kellosalo, J., Kajander, T., Kogan, K., Pokharel, K., and Goldman, A. (2012) The structure and catalytic cycle of a sodium-pumping pyrophosphatase. *Science* 337: 473–476.

Kriegel, A. Adres, Z., Medzhradszky, A., Kruger, F. Scholl, S., Delange, S., et al. (2015) Job shareing in the endomembrane system: vacuolar acidification requires the combined activity of V-ATPase and V-PPase. *Plant Cell* 27: 3383–3396.

Langhans, M., Ratajczak, R., Lützelschwab, M., Michalke, W., Wächter, R., Fischer-Schliebs, E., et al. (2001) Immunolocalization of plasma-membrane H^+-ATPase and tonoplast-type pyrophosphatase in the plasma membrane of the sieve element-companion cell complex in the stem of *Ricinus communis* L. *Planta* 213: 11–19.

Lee, C.H., Pan, Y.J., Huang, Y.T., Liu, T.H., Hsu, S.H., Lee, C.H., et al. (2011) Identification of essential lysines involved in substrate binding of vacuolar H^+-pyrophosphatase. *J. Biol. Chem.* 286: 11970–11976.

Lerchl, J., Geigenberger, P., Stitt, M., and Sonnewald, U. (1995) Impaired photoassimilate partitioning caused by phloem-specific removal of pyrophosphate can be complemented by a phloem-specific cytosolic yeast-derived invertase in transgenic plants. *Plant Cell* 7: 259–270.

Li, J., Yang, H., Peer, W.A., Richter, G., Blakeslee, J., Bandyopadhyay, A., et al. (2005) *Arabidopsis* H^+-PPase AVP1 regulates auxin mediated organ development. *Science* 310: 121–125.

Li, K.M., Wilkinson, C., Kellosalo, J., Tsai, J.Y., Kajander, T., Jeuken, L.J.C., et al. (2016) Membrane pyrophosphatases from *Thermotoga maritima* and *Vigna radiata* suggest a conserved coupling mechanism. *Nature Commu.* 7: 13596.

Lin, S.M., Tsai, J.Y., Hsia, C.D., Huang, Y.T., Chiu, C.L., Liu, M.H.,Tung, J.Y., Liu, T.H. Pan, R.L., and Sun, Y.J. (2012) Crystal structure of a membrane-embedded H^+-translocating pyrophosphatase. *Nature* 484: 399–404.

Long, A.R., Williams, L.E., Nelson, S.J., and Hall, J.L. (1995) Localization of membrane pyrophosphatase activity in *Ricinus communis* seedlings. *J. Plant Physiol.* 146: 629–638.

Maeshima, M. (1990a) Development of vacuolar membranes during elongation of cells in mung bean hypocotyls. *Plant Cell Physiol*. 31: 311–317.

Maeshima, M. (1990b) Oligomeric structure of H^+-translocating inorganic pyrophosphatase of plant vacuoles. *Biochem. Biophys. Res. Commun.* 168: 1157−1162.

Maeshima, M., and Yoshida, S. (1989) Purification and properties of vacuolar membrane proton-translocating inorganic pyrophosphatase from mung bean. *J. Biol. Chem.* 264, 20068–20073.

Maeshima, M. (2000) Vacuolar H^+-pyrophosphatase. *Biochim. Biophys. Acta – Biomembrane* 1465: 37−51.

Maeshima, M. (2001) Tonoplast transporters: organization and function. *Annu. Rev. Plant Physiol. Plant Mol. Biol.* 52, 469-497

Martinoia, E., Maeshima, M., and Neuhaus, E. (2007) Vacuolar transporters and their essential role in plant metabolism. *J. Exp. Bot.* 58: 83−102.

Mimura, H., Nakanishi, Y., Hirono, M., and Maeshima, M. (2004) Membrane topology of the H^+-pyrophosphatase of *Streptomyces coelicolor* determined by cysteine-scanning mutagenesis. *J. Biol. Chem.* 279: 35106-35112.

Mimura, H., Nakanishi, Y., and Maeshima, M. (2005) Oligomerization of the H^+-pyrophosphatase and its structural and functional consequences. *Biochim. Biophys. Acta – Bioenergetics* 1708: 393–403.

Mitsuda, N., Takeyasu, K., and Sato, M.H. (2001a) Pollen-specific regulation of vacuolar H^+-PPase expression by multiple cis-acting elements. *Plant Mol. Biol.* 1: 185–192.

Mitsuda, N., Enami, K., Nakata, M., Takeyasu, K., and Sato, M.H. (2001b) Novel type *Arabidopsis thaliana* H^+-PPase is localized to the Golgi apparatus. *FEBS Lett.* 488: 29–33.

Muto, Y., Segami, S., Hayashi, H., Sakurai, J., Murai, M., Hattori, Y., et al. (2011) Vacuolar proton pumps and aquaporins involved in rapid internode elongation of deepwater rice. *Biosci. Biotechnol. Biochem.* 75: 114–122.

Nakanishi, Y., and Maeshima, M. (1998) Molecular cloning of vacuolar H^+-pyrophosphatase and its developmental expression in growing hypocotyl of mung bean. *Plant Physiol.* 116: 589–97.

Nakanishi, Y., Saijo, T., Wada, Y., and Maeshima, M. (2001) Mutagenic analysis of functional residues in putative substrate binding site and acidic regions of vacuolar H^+-pyrophosphatase. *J. Biol. Chem.* 276: 7654–7660.

Nakanishi, Y., Yabe, I., and Maeshima, M. (2003) Patch clamp analysis of H^+ pump expressed in giant yeast vacuoles. *J. Biochem.* 134: 615–623.

Navarro-De la Sancha, E., Coello-Coutiño, M.P., Valencia-Turcotte, L.G., Hernández-Domínguez, E.E., Trejo-Yepes, G., et al. (2007) Characterization of two soluble inorganic pyrophosphatases from *Arabidopsis thaliana*. *Plant Sci.* 172: 796–807.

Nyren, P., Hajnal, K., and Baltscheffsky, M. (1984) Purification of the membrane-bound proton-translocating inorganic pyrophosphatase from *Rhodospirillum rubrum*. *Biochim. Biophys. Acta* 766: 630–635.

Paez-Valencia, J., Patron-Soberano, A., Rodriguez-Leviz, A., Sanchez-Lares, J., Sanchez-Gomez, C., Valencia-Mayoral, P., et al. (2011) Plasma membrane localization of the type I H^+-PPase AVP1 in sieve element-companion cell complexes from *Arabidopsis thaliana*. *Plant Sci*. 181: 23–30.

Palmgren, M.G., and Nissen, P. (2011) P-type ATPases. *Annu. Rev. Biophys.* 40: 243–266.

Pan, Y.J., Lee, C.H., Hsu, S.H., Huan, Y.T., Lee, C.H., Liu, T.H., et al. (2011) The transmembrane domain 6 of vacuolar H^+-pyrophosphatase mediates protein targeting and proton transport. *Biochim. Biophys. Acta* 1807: 59–67

Pedersen, B.P., Buch-Pedersen, M.J., Morth, J.P., Palmgren, M.G., and Nissen, P. (2007) Crystal structure of the plasma membrane proton pump. *Nature* 450: 1111-1115.

Pérez-Castiñeira, J.R., Hernández, A., Drake, R., and Serrano, A. (2011). A plant proton-pumping inorganic pyrophosphatase functionally complements the vacuolar ATPase transport activity and confers bafilomycin resistance in yeast.

Biochem. J. 437: 269–278.
Pizzio, G. Paez-Valencia, J., Khadilkar, A.S., Regmi, K., Patron-Soberano, A., Zhang, S., et al. (2015) Arabidopsis type I proton-pumping pyrophosphatase expresses strongly in phloem, where it is required for pyrophosphate metabolism and photosynthate partitioning. *Plant Physiol.* 167: 1541–53.
Rea, P.P., and Poole, R.J. (1986) Chromatographic resolution of H^+-translocating pyrophosphatase from H^+-translocating ATPase of higher plant tonoplast. *Plant Physiol.* 81: 126–129.
Regmi, K.C., Zhang, S., and Gaxiola, R.A. (2016) Apoplasmic loading in the rice phloem supported by the presence of sucrose synthase and plasma membrane-localized proton pyrophosphatase. *Annals Bot.* 117: 257–268.
Robinson, D.G. (1996). Pyrophosphatase is not (only) a vacuolar marker. *Trends Plant Sci.* 1: 330.
Sarafian, V., Kim, Y., Poole, R.J., and Rea, P.A. (1992) Molecular cloning and sequence of cDNA encoding the pyrophosphate energized vacuolar membrane proton pump of *Arabidopsis thaliana*. *Proc Natl Acad Sci USA* 89: 1775–1779.
Sato, M., Maeshima, M., Ohsumi, Y., and Yoshida, M. (1991) Dimeric structure of H^+-translocating pyrophosphatase from pumpkin vacuolar membranes. *FEBS Lett.* 290: 177–180.
Segami, S., Nakanishi, Y., Sato, M.H., and Maeshima, M. (2010) Quantification, organ-specific accumulation and intracellular localization of type II H^+-pyrophosphatase in *Arabidopsis thaliana*. *Plant Cell Physiol*. 51: 1350–1360.
Segami, S., Makino, S., Miyake, A., Asaoka, M., and Maeshima, M. (2014) Dynamics of vacuoles and H^+-pyrophosphatase visualized by monomeric green fluorescent protein in *Arabidopsis*: artifactual bulbs and native intravacuolar spherical structures. *Plant Cell* 26: 3416–3434.
Seufferheld, M.J., Kim, K.M., Whitfield, J., Valerio, A., and Caetano-Anollés, G. (2011) Evolution of vacuolar proton pyrophosphtase domains and volutin granules: clues into the early evolutionary origin of the acidocalcisome. *Biology Direct* 6: 50.
Schilling, R.K., Marschner, P., Shavrukov, Y., Berger, B., Tester, M., Roy, S.J., et al. (2014) Expression of the *Arabidopsis* vacuolar H^+-pyrophosphatase gene (AVP1) improves the shoot biomass of transgenic barley and increases grain yield in a saline field. *Plant Biotech. J*. 12: 378–386.
Schulze, S., Mant, A., Kossmann, J., and Lloyd, J.R. (2004) Identification of an Arabidopsis inorganic pyrophosphatase capable of being imported into chloroplasts. *FEBS Lett.* 565: 101–105.
Schumacher, K. (2014) pH in the plant endomembrane system – an import and export business. *Curr. Opin. Plant Biol.* 22: 71–76.
Shen, J., Zeng, Y., Zhuang, X., Sun, L., Yao, X., Pimpl, P., et al. (2013) Organelle pH in the *Arabidopsis* endomembrane system. *Mol. Plant* 6: 1419–1437.
Sivula, T., Salminen, A., Parfenyev, A.N., Pohjanjoki, P., Goldman, A., Cooperman, B.S., et al. (1999) Evolutionary aspects of inorganic pyrophosphatase. *FEBS Lett.* 454: 75–80.

Sze, H., Schumacher, K., Müller, M.L., Padmanaban, S., and Taiz, L. (2002) A simple nomenclature for a complex proton pump: VHA genes encode the vacuolar H^+-ATPase. *Trend Plant Sci.* 7: 157–161.

Takahashi, K., Morimoto, R., Ishida, M., Asaoka, M., Maeshima, M., Tsukaya, H., et al. (2017) Compensated cell enlargement in *fugu5* is specifically triggered by lowered sucrose production from seed storage lipids. *Plant Cell Physiol.* 58: 668–678.

Takeshige, K., Tazawa, M., and Hager, A. (1988) Characterization of the H^+ translocating adenosine triphosphatase and pyrophosphatase of vacuolar membranes isolated by means of a perfusion technique from *Chara corallina*. *Plant Physiol*. 86: 1168–1173.

Ueoka-Nakanishi, H., and Maeshima, M. (2000) Quantification of Ca^{2+}/H^+ antiporter VCAX1p in vacuolar membranes and its absence in roots of mung bean. *Plant Cell Physiol.* 41: 1067–1071.

Vitha, S., Yang, M., Sack, F.D., and Kiss, J.Z. (2007) Gravitropism in the *starch excess* mutant of *Arabidopsis thaliana*. *Amer. J. Bot*. 94: 590–598.

Wang, X., Wang, H., Liu, S., Ferjani, A., Li, J., Yan, J., et al. (2016) Genetic variation in ZmVPP1 contributes to drought tolerance in maize seedlings. *Nature Genet.* 48: 1233–1241.

Figure legends

Figure 1. Visualisation of vacuolar H^+-PPase (V-PPase) in seedlings by expression of V-PPase tagged with the monomeric form of green fluorescent protein (mGFP). (A) V-PPase-mGFP was expressed in *Arabidopsis thaliana*. An etiolated transgenic 3.5-day-old seedling was observed with a stereo microscope (left panel) and a confocal laser scanning microscope (right panel). Arrows indicate parts with high intensity of V-PPase-mGFP fluorescence: a, cotyledons; b, hook (elongation region); c, root-shoot boundary region; and d, root meristematic region except for the quiescent center. (B) Fluorescence image of seedling root expressing V-PPase-mGFP. Seedling was stained with propidium iodide (PI) to visualise the cell wall (purple; right panel).

Figure 2. Tertiary structure of V-PPase of *Vigna radiata*. Lin et al. (2012) revealed the crystal structure of *V*. *radiata* V-PPase, which exists as a homodimer. (A and B) Three-dimensional images of V-PPase from the cytoplasmic side (A) and the side view (B) taken from the RCSB Protein Data Bank (rcsb.org; 4A01), which is based on published data (Lin et al. 2012). (C) Schematic representation of the top view of the V-PPase dimer to show arrangement of the transmembrane helices (TM1–TM16). TM helices in the inner and outer rings are shown in light brown and blue, respectively. (D) A schematic model of the functional domains for substrate hydrolysis, energy transfer, H^+ translocation, and H^+ release based on previous reports (Lin et al. 2012, Kellosalo et al. 2012, Li et al. 2016).

Figure 3. Inorganic pyrophosphate (PPi)-dependent H^+ current detected by patch clamp analysis of V-PPase expressed in a giant yeast vacuole. (A) Adenosine triphosphate (ATP)- and PPi-induced currents in an intact vacuole expressing *V*. *radiata* V-PPase. Both the bathing (cytoplasmic side) and pipette solutions (vacuolar lumen side) contained the appropriate buffer, 0.1 M KCl, and 1 mM $MgCl_2$. The substrate, ATP (1 mM; at 1 and 13 min) or PPi (0.2 mM; at 7 min), was applied to the bathing solution at the indicated time for 3 min. The current of endogenous V-type H^+-ATPase (V-ATPase) was observed. (B) The H^+ current was monitored using a single vacuole with the indicated concentrations of PPi. Inserted table shows the final total concentrations of PPi and calculated concentrations of Mg_2PPi in parentheses. The calculated K_m for Mg_2PPi was 4.6 μM. Data are from Nakanishi et al. (2003).

Figure 4. Ability of V-PPase to acidify the vacuole. A model vacuole with a diameter of 10 μm is shown. The total number of protons are calculated to be 3.2×10^4 at pH 7.0 and 3.2×10^5 at pH 6.0 in this vacuole (5.2×10^{-13} L in volume). Overall, 2.9×10^5 protons are required to acidify the vacuole from pH 7.0 to 6.0. The plant vacuole is estimated to contain 1–7.5×10^5 dimers of V-PPase and each dimer actively translocates protons at a velocity of 28 s^{-1} (see text). Thus, it is not a heavy load for V-PPase to acidify the vacuole and maintain the acidity. V-ATPase consists of multiple subunits and its total molecular mass is more than 760 kDa (Sze et al.

2002). The apparent turnover number of V-ATPase is 90 H^+ s^{-1} (ATP hydrolysis, 45 s^{-1}) (Ueoka-Nakanishi et al. 2000).

Figure 1

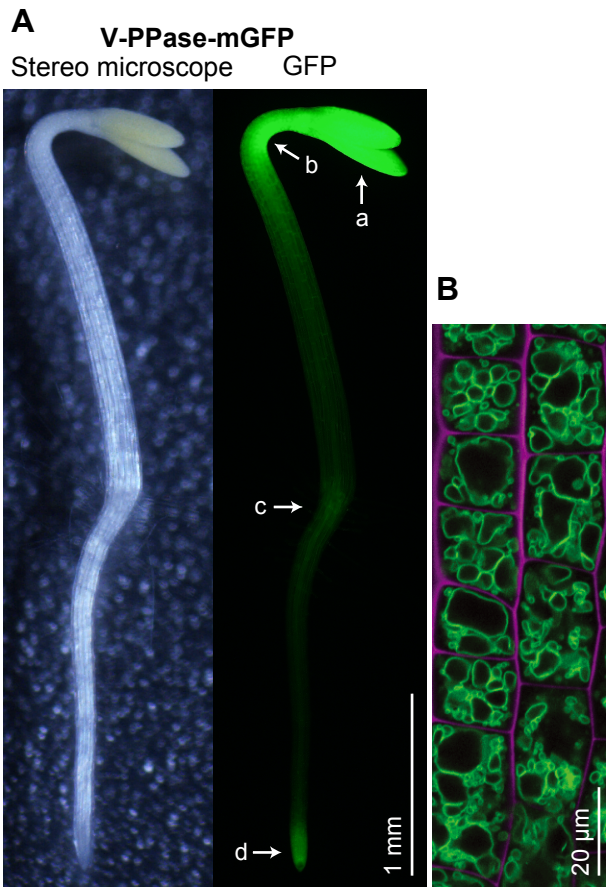

Figure 2 (Maeshima)

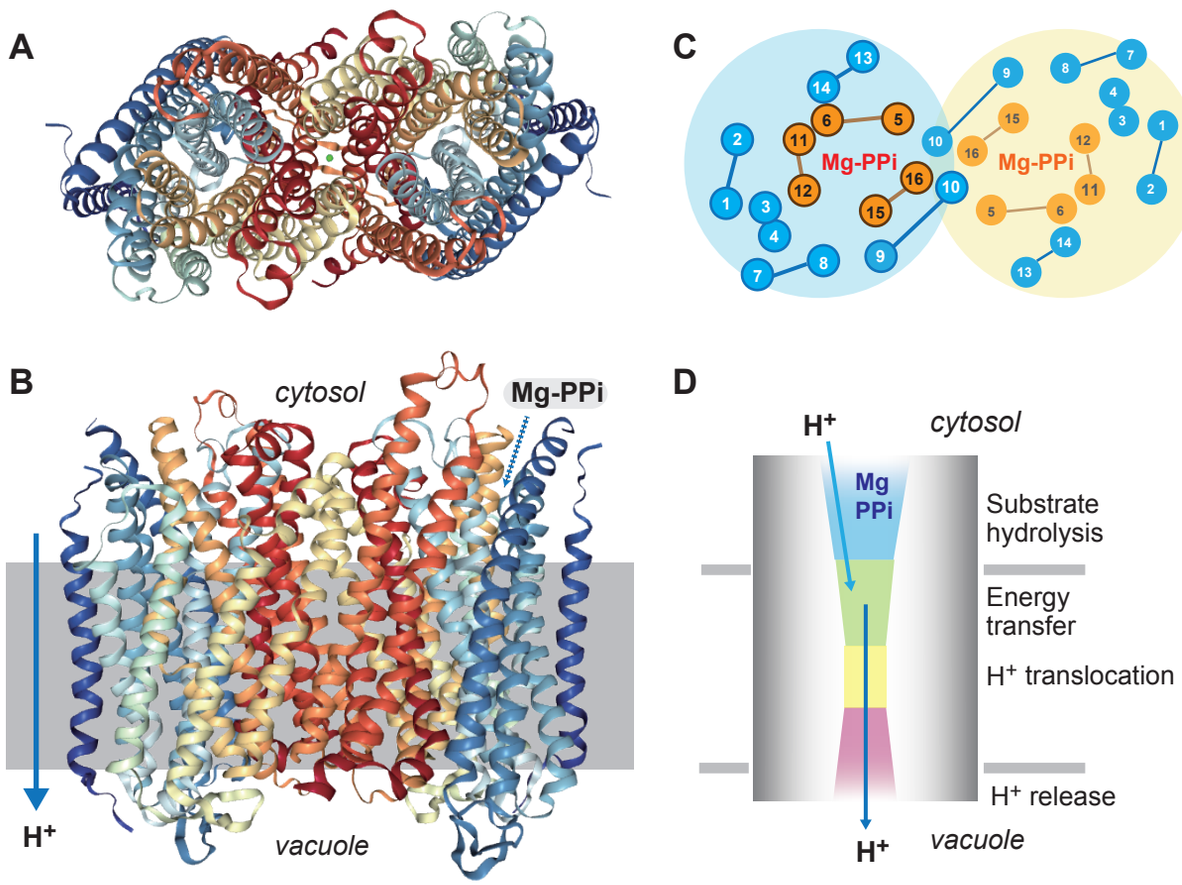

Figure 3

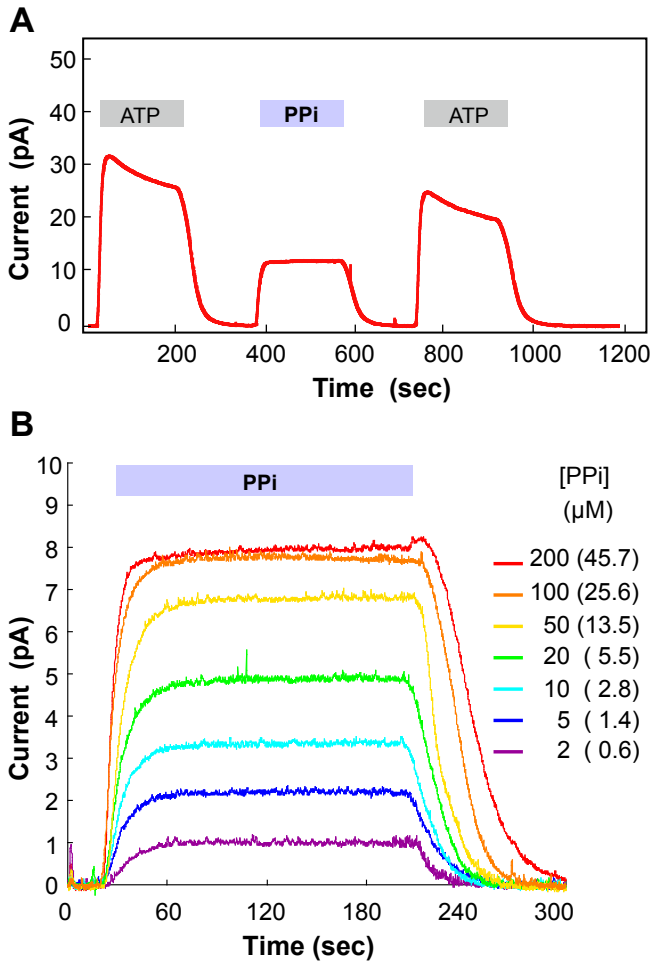
A
ATP
PPi
ATP
Current (pA)
Time (sec)
B
PPi
[PPi]
(μM)
200 (45.7)
100 (25.6)
50 (13.5)
20 (5.5)
10 (2.8)
5 (1.4)
2 (0.6)
Current (pA)
Time (sec)

Figure 4 (Maeshima)